The EMBO Journal vol.14 no.4 pp.842–852, 1995

Structural and functional studies of retroviral RNA pseudoknots involved in ribosomal frameshifting: nucleotides at the junction of the two stems are important for efficient ribosomal frameshifting

Xiaoying Chen[1], Mario Chamorro[2,3], Susanna I.Lee[3,4], Ling X.Shen[1], Jennifer V.Hines[1,5], Ignacio Tinoco,Jr[1] and Harold E.Varmus[2,3]

[1]Department of Chemistry and Laboratory of Chemical Biodynamics, University of California, Berkeley, CA 94720, [2]National Cancer Institute, NIH, Bethesda, MD 20892, [3]Department of Microbiology and Immunology and Biochemistry and Biophysics, University of California, San Francisco, CA 94143, [4]Miriam Hospital, Brown University, 164 Summit Avenue, Providence, RI 02906 and [5]Department of Chemistry, Kenyon College, Gambier, OH 43022, USA

Y.Chen and M.Chamorro contributed equally to this work

Communicated by H.E.Varmus

Ribosomal frameshifting, a translational mechanism used during retroviral replication, involves a directed change in reading frame at a specific site at a defined frequency. Such programmed frameshifting at the mouse mammary tumor virus (MMTV) *gag-pro* shift site requires two mRNA signals: a heptanucleotide shifty sequence and a pseudoknot structure positioned downstream. Using *in vitro* translation assays and enzymatic and chemical probes for RNA structure, we have defined features of the pseudoknot that promote efficient frameshifting. Heterologous RNA structures, e.g. a hairpin, a tRNA or a synthetic pseudoknot, substituted downstream of the shifty site fail to promote frameshifting, suggesting that specific features of the MMTV pseudoknot are important for function. Site-directed mutations of the MMTV pseudoknot indicate that the pseudoknot junction, including an unpaired adenine nucleotide between the two stems, provides a specific structural determinant for efficient frameshifting. Pseudoknots derived from other retroviruses (i.e. the feline immunodeficiency virus and the simian retrovirus type 1) also promote frameshifting at the MMTV *gag-pro* shift site, dependent on the same structure at the junction of the two stems.

Key words: frameshifting/nickel complex/pseudoknot/retrovirus

Introduction

In retroviruses the *pol* (or *pro/pol*) gene encodes three essential enzymes: integrase, protease and reverse transcriptase. These gene products are expressed from a polycistronic mRNA and are regulated at the level of translation, by either ribosomal frameshifting into the −1 frame or read-through of a termination codon (for reviews see Atkins *et al.*, 1990; Jacks, 1990; Hatfield *et al.*, 1991). It has been demonstrated that several organisms and genetic elements other than retroviruses also regulate the expression of their genes by ribosomal frameshifting. These include coronaviruses (Brierley *et al.*, 1989; Bredenbeek *et al.*, 1990; den Boon *et al.*, 1991; Herold and Siddell, 1993), toroviruses (Snijder *et al.*, 1990), the yeast LA double-stranded (ds) RNA virus (Dinman *et al.*, 1991; Tzeng *et al.*, 1992), the yeast retrotransposon *Ty* (Clare and Farabaugh, 1985; Mellor *et al.*, 1985) and several prokaryotes (Craigen and Caskey, 1987; Sekine *et al.*, 1989; Flower *et al.*, 1990; Tsuchihashi *et al.*, 1990).

Jacks *et al.* (1988) established that when translating Rous sarcoma virus (RSV) RNA, the ribosome shifts into the −1 reading frame at the *gag-pol* overlap in response to at least two sets of *cis*-acting signals in the viral mRNA: a consensus heptanucleotide sequence and a higher order RNA structure downstream of this shift site. In a more comprehensive mutational analysis of the open reading frame (ORF) *1a* and *1b* overlap region of the coronavirus infectious bronchitis virus (IBV), Brierley *et al.* (1989, 1991) showed that the downstream RNA structure is composed of two stems that, if formed simultaneously, would fold into a pseudoknot structure. A survey of many retroviral RNAs has revealed sequences consistent with pseudoknotted RNA structures downstream of many demonstrated or suspected frameshift sites (ten Dam *et al.*, 1990).

The mechanism by which a pseudoknot promotes ribosomal frameshifting is unknown. It was proposed by Jacks *et al.* (1988) that RNA structure may cause pausing of the ribosome at the shift site and thereby induce slippage into the −1 reading frame. Ribosomal pausing has been observed at a few shift sites: the *Escherichia coli dnaX* gene (Tsuchihashi, 1991), the LA dsRNA virus (Tu *et al.*, 1992) and the IBV mRNA (Somogyi *et al.*, 1993). In the latter two cases, a pseudoknot is located downstream of the shift site. However, a simple stem−loop in IBV, which is unable to direct efficient frameshifting, also causes ribosomal pausing, though at a reduced level, suggesting that factors other than the ability of pseudoknots to impede ribosomal progression are important in frameshifting (Somogyi *et al.*, 1993). Thus, the idea that a pseudoknot serves simply as an energetic barrier to the ribosome does not provide a satisfactory explanation of how the RNA structure promotes frameshifting. These results suggest that a particular conformational feature of the pseudoknot is important for its ability to promote frameshifting. Clearly, more information on the structure and thermodynamics of pseudoknots is needed before we can fully understand their role in frameshifting events.

The highly efficient ribosomal frameshifting in the *gag-pro* overlapping region of mouse mammary tumor virus (MMTV) mRNA requires a pseudoknot (Figure 1; Chamorro *et al.*, 1992). Mutations that disrupt the base pairing in either stem 1 or stem 2 of the pseudoknot impair frameshifting, while compensatory changes that

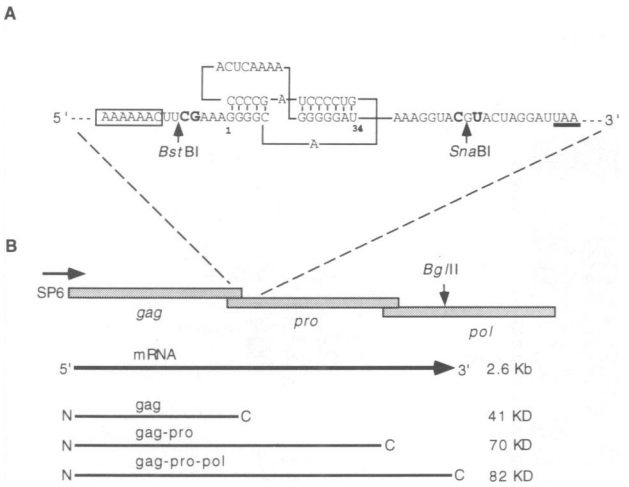

Fig. 1. Predicted RNA pseudoknot at the MMTV *gag-pro* frameshift site. (**A**) The predicted secondary structure of the MMTV pseudoknot is shown downstream of the frameshift site, the boxed heptanucleotide AAAAAAC. The nucleotides in bold were mutated from the wild-type sequence to create two unique restriction sites, *Bst*BI and *Sna*BI, which are indicated by arrows. As a result, the stop codon in the *gag* reading frame was moved from a position 5′ of the pseudoknot to the underlined UAA. (**B**) Ribosomal frameshifting assay. The plasmid pMGPP contains three overlapping MMTV reading frames: *gag*, *pro* and *pol*. Linearization of the plasmid with *Bgl*II and *in vitro* transcription using SP6 RNA polymerase yields a 2.4 kb mRNA. *In vitro* translation of the mRNA in rabbit reticulocyte lysates produces Gag (41 kDa), Gag-Pro (70 kDa) and Gag-Pro-Pol (82 kDa) fusion proteins.

restore the base pairing restore frameshifting. These results are consistent with the presence of the pseudoknot suggested by the sequence. However, the predicted RNA pseudoknot is 34 nucleotides long, with only a single nucleotide in loop 1. This contrasts with the requirement for at least two nucleotides crossing the deep and narrow major groove of an A-form helix in model pseudoknots that have been studied previously (Pleij *et al.*, 1985; Le *et al.*, 1989; ten Dam *et al.*, 1990; Wyatt *et al.*, 1990). Another unexpected feature of the MMTV pseudoknot is that an unpaired residue is predicted to separate the two stems of the pseudoknot and might compromise the coaxial stacking interactions of the two stems. These unusual structural features of the MMTV pseudoknot may play important roles in ribosomal frameshifting.

Here we report that pseudoknots downstream of retroviral shift sites display specific structural features necessary to direct efficient frameshifting. First, a simple stem−loop, a tRNA structural motif and a synthetic model pseudoknot were all shown to be inefficient in directing frameshifting. Thus the existence of a stable structure in the mRNA downstream of the shifty site is not sufficient to cause the ribosome to shift frame. To investigate further the structure−function relationship of pseudoknot-promoted frameshifting, we carried out site-directed mutagenesis on the pseudoknot in the *gag-pro* overlapping region of MMTV. The structures of the MMTV pseudoknot mutant RNAs were characterized using chemical and enzymatic probes, and correlated with their ability to promote frameshifting in a rabbit reticulocyte lysate translation system.

Our results establish that the 34 nucleotide sequence downstream of the MMTV *gag-pro* frameshift site is indeed able to form a pseudoknotted structure. The two stems of the pseudoknot are separated by a single nucleotide at the junction, and this nucleotide interrupts the coaxial stacking of the two helices. The junction region between the two stems was found to be a major structural feature that determines the ability of the pseudoknot to promote frameshifting. Furthermore, other retroviral pseudoknots that direct frameshifting on feline immunodeficiency virus (FIV) and simian retrovirus (SRV-1) RNA (ten Dam *et al.*, 1990; Morikawa and Bishop, 1992) are also efficient in promoting frameshifting when placed in the context of MMTV RNA. Although the stems and loops of these pseudoknots differ from those of the MMTV pseudoknot, the junctions between the stems are very similar and are also required for efficient frameshifting, thereby revealing a common structural determinant among the retroviral pseudoknots that facilitate −1 frameshifting.

Results

Our strategy for the analysis of the structure−function relationship of pseudoknot-promoted frameshifting by retroviruses was: (i) to map the structure of the pseudoknot in the *gag-pro* overlapping region of MMTV with the use of chemical and enzymatic probes, (ii) to create defined structural mutations within the pseudoknot, and (iii) to assay these changes for frameshifting function in a rabbit reticulocyte lysate translation system.

Mapping of the MMTV pseudoknot structure

Our previous mutational studies strongly suggested that a 34 nucleotide sequence, starting seven nucleotides downstream of the MMTV *gag-pro* frameshift site, forms a pseudoknotted RNA structure, which is necessary for high levels of frameshifting (Chamorro *et al.*, 1992; Figure 1). To facilitate structural studies on the predicted MMTV pseudoknot by chemical and enzymatic probes (and for use in studies by NMR, to be reported elsewhere), an RNA pseudoknot oligonucleotide (VPK, 34 nucleotides; Figure 2) was synthesized *in vitro* by T7 RNA polymerase (Milligan *et al.*, 1987; Wyatt *et al.*, 1991). This pseudoknot differs from the wild-type pseudoknot in that G·C base pairs were flipped in stem 1 and in stem 2 (Figure 3A). When introduced in the mRNA, VPK preserves the same frameshifting efficiency (12%) as the wild-type pseudoknot in the context of the *Bst*BI−*Sna*BI sites flanking the pseudoknot region that were introduced to simplify the construction of mutants (Figure 3B).

Single-strand (ss) and double-strand (ds)-specific enzymes (Puglisi *et al.*, 1990) and a base-specific metal complex (Chen *et al.*, 1993) were used to probe the structure of the 34 nucleotide VPK RNA oligonucleotide (Figure 2). The ds-specific ribonuclease, V_1, cleaves efficiently in the stem regions of VPK as well as loop 1, while the ss-specific nuclease, S_1, cleaves predominantly in the loop 2 region and mildly in the lower part of stem 2 (Figure 2). This is consistent with the structural studies of pseudoknots reported previously: nucleotides in loop 2, which bridge the shallow minor groove, are more accessible to ss-specific probes than those in loop 1 (van Belkum *et al.*, 1988; Puglisi *et al.*, 1990). Base stacking interactions of the nucleotides in loop 1, as indicated by NMR data (unpublished results), make them accessible to

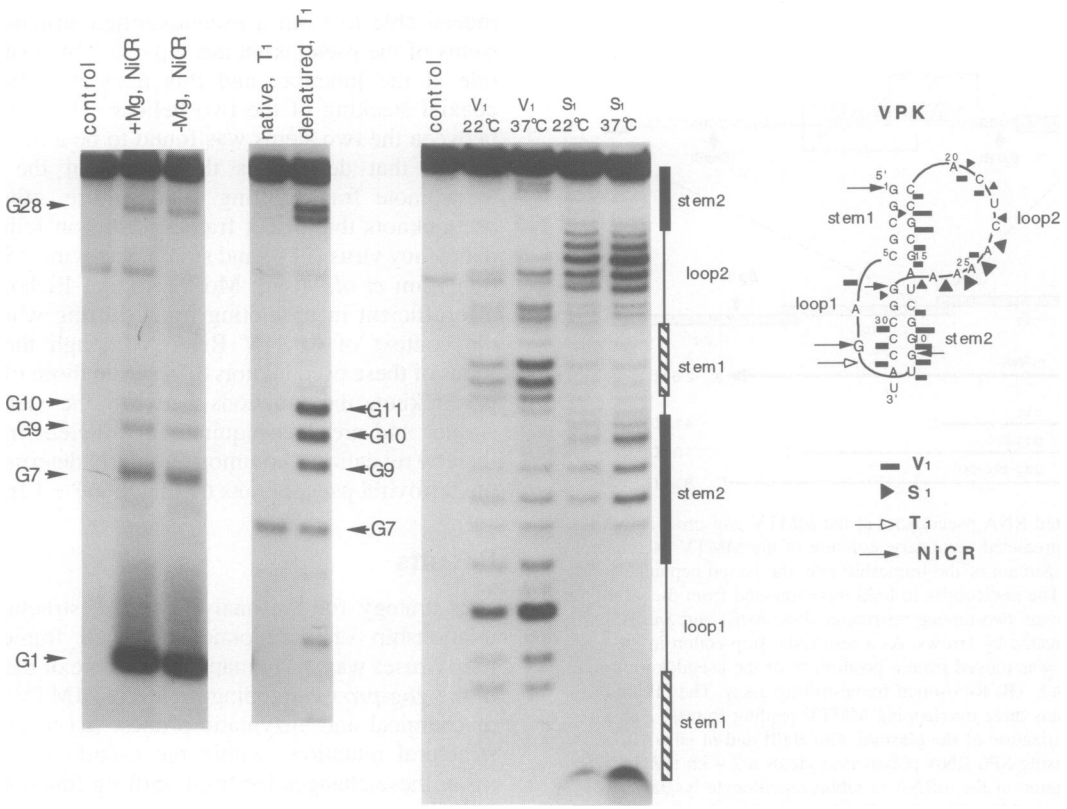

Fig. 2. Structural mapping of an RNA pseudoknot. Autoradiograms are shown with partial digestion products of the VPK oligoribonucleotide by nucleases S_1, V_1 and T_1, and by a chemical probe, NiCR (see Materials and methods). The RNA was ^{32}P-labeled at the 5′ end. The vertical bars to the right of the autoradiograms indicate the predicted positions of the stems and loops of VPK. The numbering on the two left-most panels indicates the positions of the fragments obtained after RNase T_1 and NiCR cleavage. On the far right, a schematic representation of the folded VPK oligoribonucleotide is shown. Enzymatic and chemical cleavage sites are indicated.

V_1 cleavage. The ss, G-specific RNase T_1 nuclease cleaves primarily at G7 (Figure 2), indicating that the predicted G7·U34 base pairing (see Figure 1; ten Dam *et al.*, 1990) does not occur. Thus, loop 1 is actually two nucleotides in length, consistent with the requirement that at least two nucleotides are necessary to cross the deep major groove of stem 2 (Figure 2).

A more detailed analysis was carried out by a conformation-sensitive chemical probe, NiCR/[2,12-dimethyl-3,7,11,17-tetraazabicyclo(11.3.1)heptadeca-1(17),2,11,13,15-pentaene]-nickel(II) perchlorate, which cleaves at the most solvent-accessible guanines on DNA and RNA molecules (Chen *et al.*, 1992, 1993). There was no difference in cleavage with NiCR in the presence or absence of magnesium (Figure 2), indicating that this pseudoknot can be stabilized at 100 mM NaCl without magnesium. G1 and G7 were cleaved most efficiently, followed by G9 and G28 (Figure 2). The cleavage of G7 and G9 further confirms the assignment of G7 to loop 1, and the mild cleavage at G28 indicates that this base is located at the junction of stem 2 and loop 2.

Substitution of the MMTV pseudoknot with a stem–loop, tRNA and PK5

There are two general models for the role of pseudoknots in frameshifting. One is that the pseudoknot is recognized by a component of the translation apparatus and thereby signals the ribosome to shift into the −1 frame. Alternatively, the RNA pseudoknot may serve as a 'roadblock' that resists the unwinding of the RNA structure during translation and thereby causes the ribosome to pause over the shift site. This latter model predicts that any RNA motif which forms a stable mRNA structure may stall the motion of the ribosome and promote the −1 frameshift. To distinguish between these two models, we substituted various heterologous RNA structures (i.e. a stem–loop, a tRNA and a synthetic pseudoknot) for the pseudoknot downstream of the MMTV *gag-pro* frameshift site.

We first asked whether the stability of a downstream structure was its only relevant feature for directing frameshifting. A stem–loop is predicted to be more stable than a pseudoknot of the same length and base pair composition. A hairpin composed of both stems of VPK joined by the unpaired A14 was constructed (Figure 3A, HP). This hairpin, which is of high predicted thermodynamic stability ($\Delta G° \approx -18$ kcal/mol at 37°C; Jaeger *et al.*, 1989), displayed low frameshifting efficiency (Figure 3B, 2%) relative to VPK (Figure 3B, 12%).

To strengthen the argument that any stable mRNA structure is not sufficient to direct efficient frameshifting, we substituted $tRNA^{phe}$, of greater structural complexity and stability than VPK, downstream of the MMTV shift site (Figure 3A, $tRNA^{phe}$). It has been confirmed that unmodified $tRNA^{phe}$ can be aminoacylated efficiently by the tRNA synthetase, and that it is folded normally to the L-shaped tertiary structure (Sampson and Uhlenbeck,

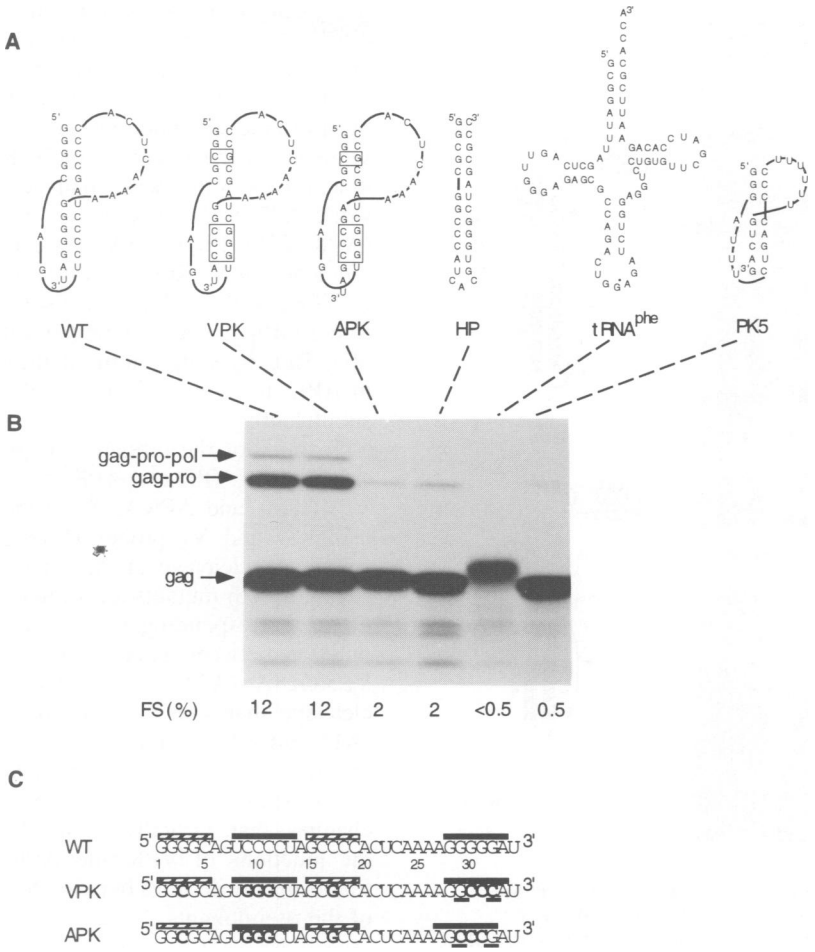

Fig. 3. An RNA pseudoknot with special structural features is required for efficient frameshifting. (**A**) Schematic representation of three related pseudoknots (WT, VPK and APK), an unrelated pseudoknot (PK5), a hairpin (HP) and a tRNA (tRNA^{phe}) in the context of MMTV *gag-pro* mRNA. These sequences were introduced into MMTV RNA by site-directed mutagenesis of the MMTV DNA, as described in Materials and methods. The boxed sequences in VPK and APK show nucleotides that differ from WT. The residue *G in tRNA^{phe} was changed from A to G to avoid a UGA stop codon in the *gag* reading frame. (**B**) Reticulocyte lysate translation products. Positions of [^{35}S]methionine-labeled products of translation in a 10% SDS–polyacrylamide gel are indicated to the left of the autoradiogram, and the computed ribosomal frameshifting efficiencies are listed below each lane (experimental variation ± 1%). (**C**) Linear sequences, given 5′ to 3′, of the three related pseudoknots depicted in (A). The hatched boxes above particular bases indicate their participation in forming stem 1. The solid black boxes above particular bases indicate their participation in forming stem 2. The bold face indicates bases mutated to form the related pseudoknots VPK and APK. The underlined bases represent the bases that differ between VPK and APK.

1988). The replacement of the VPK pseudoknot with tRNA^{phe} reduced the frameshifting efficiency to undetectable levels (Figure 3B). The slowly migrating Gag protein in the gel (Figure 3B, compare VPK with tRNA^{phe}) indicates that ribosomes are able to read through the tRNA structure, since the stop codon of the *gag* reading frame is downstream from the tRNA in this construct. Thus, the stability of the downstream structure is not the only determinant for directing efficient frameshifting.

These results argue that the pseudoknot displays specific structural features that direct the ribosome to shift frame. To test whether a frameshifting pseudoknot contains unique structural motifs in addition to a general pseudoknot conformation, we introduced the model pseudoknot, PK5, whose structure has been studied by NMR (Puglisi *et al.*, 1990). As shown in Figure 3, PK5 directs frameshifting very poorly (0.5%). Thus, PK5 lacks structural features contained in VPK for directing efficient frameshifting.

Structural comparisons of two similar pseudoknots with different frameshifting efficiencies reveal differences at the junction of the two stems

As discussed earlier, the predicted conformation of VPK is similar to wild-type except for the flipping of G·C base pairs in stems 1 and 2. We also constructed another mutant, APK, which maintains the same exchange of bases in stem 1 but has further alterations in stem 2. These changes would cause a predicted shift in the base pairing of stem 2 so that an A27·U13 pair becomes the top of stem 2, thereby shortening loop 2 from eight to seven nucleotides (see Figure 3A and C). APK (Figure 3A) reduced the frameshifting efficiency to 2% (Figure 3B). Since VPK and APK have similar sequences and base pair compositions but differ in their abilities to direct frameshifting, our results suggest that the −1 frameshifting efficiency is sensitive to the detailed structural motifs in the downstream pseudoknot.

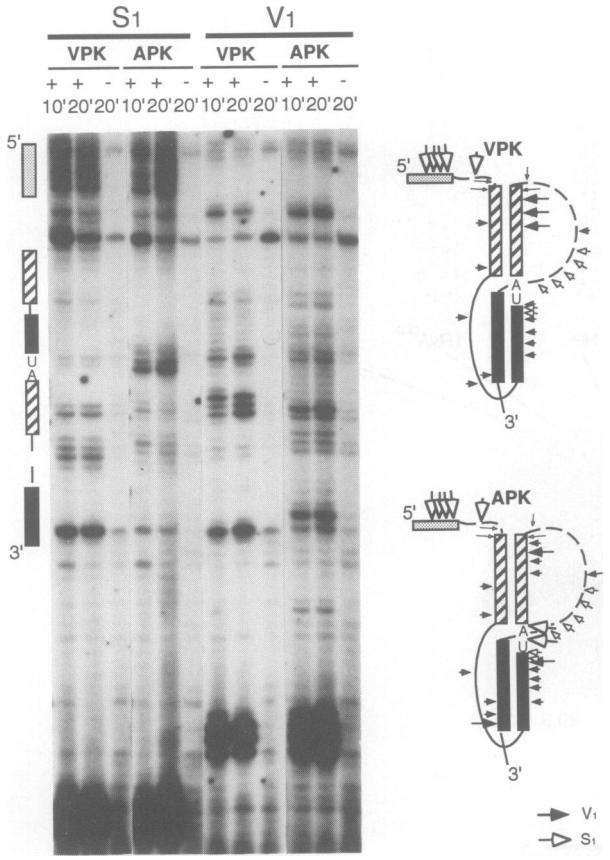

Fig. 4. Partial digestions of VPK and APK by S_1 and V_1 in the context of the MMTV mRNA. On the far left, the shift site is represented by the dotted box, stem 1 by the hatched boxes, stem 2 by the black boxes, loop 1 by the solid line and loop 2 by the dotted line. A14 at the junction and the adjacent U13 are shown. The autoradiogram was generated by RT primer extension of S_1 and V_1 digests of VPK and APK mRNAs with or without nucleases (+/−) at different time points. To the far right, the proposed folding of sequences is shown, with enzymatic cleavage sites indicated.

We compared the structures of VPK and APK in the context of MMTV mRNA by probing the full-length transcripts with S_1 and V_1 nucleases. Cleavage sites were mapped by a primer extension assay (Stern *et al.*, 1988). V_1 cleavage in the stem regions and S_1 cleavage in the loop regions of VPK and APK are consistent with pseudoknotted conformations of these sequences in the mRNA context (Figure 4). The cleavage pattern of VPK is very similar to that of APK in the stems and loops. However, there were significant differences between APK and VPK in the cleavage pattern of S_1 at nucleotides in the junction region between stem 1 and stem 2. S_1 cleaved efficiently after A14 at the junction and after the adjacent U13 in APK, while the corresponding positions in VPK were not susceptible to cleavage (see Figure 3C for sequence details). Thus, the S_1 cleavage pattern reveals structural differences in the junction regions between stems 1 and 2 of the pseudoknots, and sets the stage for investigating how the sequence and structure at the junction influences the function of pseudoknots in frameshifting.

Junction swapping between VPK and APK

Structural comparisons of the two pseudoknots, VPK and APK, revealed differences in the junction regions of the two pseudoknots. These differences might account for the different frameshifting efficiencies. Thus, swapping the junctions of VPK and APK should modulate the ability of each to promote frameshifting. We tested this hypothesis by introducing mutations that exchange the primary sequence at the junctions of VPK and APK: G28 at the junction of VPK was changed to an A (VPKG28A), while A27 at the junction of APK was changed to a G (APKA27G) (Figure 5A). As expected, the frameshifting efficiency of VPKG28A was 3-fold lower (4%) than that of VPK, while APKA27G displayed a 4-fold increase in frameshifting when compared with that of APK (Figure 5B). Thus by simply introducing the VPK junction motif in APK, the frameshifting ability of APK was improved significantly.

To monitor the influence of junction swapping on the structures of VPK and APK, we mapped the structures of VPKG28A and APKA27G in the context of the mRNA using S_1 and V_1 probes (Figure 5C). The patterns of enzymatic cleavage at the nucleotides in the loops and stems of both mutants are similar to the cleavage patterns of the corresponding parent pseudoknots, except at the junction between stem 1 and stem 2. The junction of VPKG28A (A14 and U13) is more accessible to S_1 cleavage than that of VPK. In contrast, the nucleotides (A14 and U13) in the analogous positions of APKA27G are relatively inaccessible compared with those of APK. These studies strongly suggest that single nucleotide changes that virtually swap the primary sequence at the junctions of VPK and APK altered not only their frameshifting abilities but also the structures at the junction of the pseudoknots.

The role of the intervening nucleotide (A14) at the junction of two stems

One of the features central to the stability of a pseudoknot is that the two stems stack coaxially and form a quasi-continuous A-form helix (Pleij *et al.*, 1985; Pleij and Bosch, 1989). The coaxial stacking of the two stems of a pseudoknot was observed in PK5, a synthetic model studied by 2-D NMR spectroscopy (Puglisi *et al.*, 1990). In the MMTV pseudoknot, the intervening nucleotide, A14, separating stem 1 and stem 2 would compromise the coaxial stacking interactions. To address the role of this nucleotide in the structure and function of the VPK pseudoknot, we made a series of mutations that either delete or substitute this nucleotide with a different one. The structures of these mutants were then probed and their frameshifting ability was assayed.

Deletion of the A nucleotide that separates the two stems of VPK resulted in a dramatic conformational change from a pseudoknot to a 5′ hairpin (Figure 6A, ΔA14). This structure was suggested by probing the ΔA14 oligonucleotide with NiCR (Figure 6A, compare with VPK in Figure 2). The extensive cleavage at G9, G10 and G11 of ΔA14 by NiCR strongly suggests that these three Gs are no longer protected in stem 2 as seen in VPK, but loop out in a hairpin conformation, with A6 base pairing with U13 and G7 pairing with C12 (A6 and G7 form loop 1 in VPK; see Figure 2). The formation of a hairpin with ΔA14 was confirmed by S_1 and V_1 mapping of the sequence in the context of the mRNA; intense S_1 cleavages after nucleotides U8, G9, G10 and G11 were observed

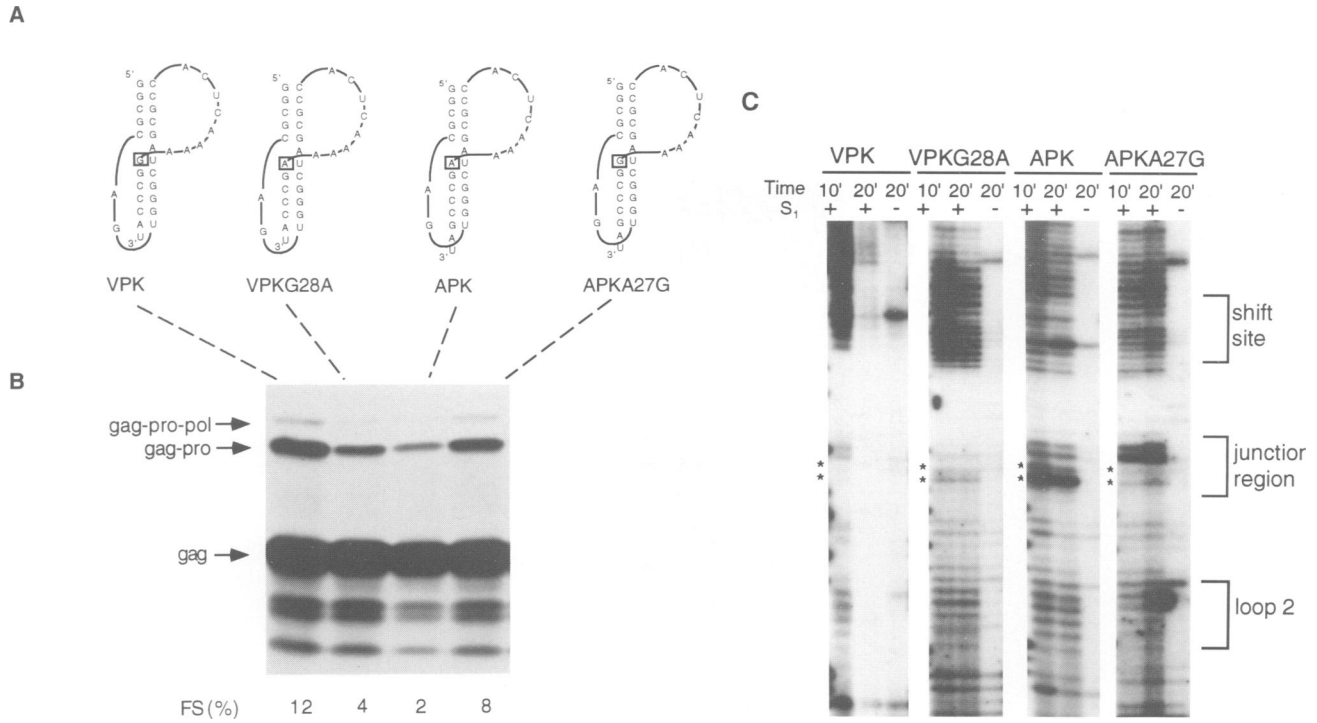

Fig. 5. Swapping the sequences at the junctions of VPK and APK changes their ability to promote frameshifting. (**A**) The sites of mutations in the junction region of the pseudoknots are boxed. (**B**) *In vitro* translation products synthesized as described in the legend to Figure 3. (**C**) Comparison of partial digestion of VPK, VPKG28A, APK and APKA27G by S_1 nuclease in the context of the MMTV mRNA. A14 and U13 are represented by '*'.

(data not shown). The thermodynamic stability of the ΔA14 oligonucleotide is predicted to be $\Delta G°$ (37°C) = −12.2 kcal/mol (Jaeger *et al.*, 1989). It has a T_m of 85°C, whereas VPK has a T_m of 72°C (determined by UV melting curves; data not shown). If the stability of the structure is the sole requirement for frameshifting, ΔA14 should promote frameshifting as well as, if not better than, the pseudoknot VPK. However, ΔA14 did not direct efficient frameshifting (Figure 6C, 2%,), as might have been predicted from the results presented in Figure 3.

To generate a pseudoknot that lacks an intervening nucleotide at the junction of the stems, U13 of VPKΔA14 was changed to a C (ΔA14U13C, Figure 6B), thereby preventing the formation of the stable stem observed in ΔA14. The pseudoknotted structure was confirmed by structural probing (data not shown). ΔA14U13C does not promote efficient frameshifting even though it forms a pseudoknot (Figure 6C, 2%). The inability of the ΔA14U13C pseudoknot to promote high efficiency frameshifting appears to be due to its structure at the junction of the stems. It lacks the A residue separating the two stems of the VPK pseudoknot. When an adenine (A14) was put back into the junction, frameshifting was restored to the wild-type level (Figure 6C, mutant U13C, 12%), confirming that the pseudoknot junction is crucial for efficient frameshifting and showing that the U13 to C change is not responsible for the impaired frameshifting by ΔA14U13C.

In the oligonucleotide pseudoknot PK5 (Puglisi *et al.*, 1990), stem 1 coaxially stacks on stem 2 to form a quasi-continuous A-form helix. This stacking between the two stems stabilizes the overall structure of the pseudoknot but imposes constraints on the two connecting loops, resulting in some distortion in the conformation at the junction. In VPK, the single adenine (A14) at the junction may serve simply to increase the distance between the two stems to avoid the unfavorable phosphate−phosphate repulsion between loop 1 and loop 2 at the junction. This predicts that increasing the distance between the stems will further release strain on the junction of the pseudoknot. To determine if such a pseudoknot will allow efficient frameshifting, we constructed a mutant of VPK with an extra nucleotide, a G, inserted in the junction (Figure 6B, A14GA). The structure of A14GA was probed with S_1, V_1 and NiCR and it is consistent with pseudoknot formation (data not shown). The extra nucleotide insertion impaired frameshifting (Figure 6C, 2%), indicating that a specific conformation at the junction of the pseudoknot, not simply disruption of coaxial stacking, is required for efficient frameshifting.

If a particular base, such as adenosine, is required to maintain a specific conformation at the junction for highly efficient frameshifting, a substitution of A14 by another nucleotide should reduce frameshifting levels. We constructed a mutant with a substitution of A14 with a G (Figure 6B, A14G). As shown in Figure 6C, the frameshifting efficiency of A14G was reduced 3-fold (4%) compared with that of VPK, indicating that the identity of the junction nucleotide is an important feature of the junction. We did not test mutants A14C or A14U. Substituting A14 with a pyrimidine would probably result in base pairing between loop 1 and the junction, as seen in ΔA14, causing a conformational change to a 5′ hairpin.

Similar pseudoknot junctions in other retroviruses

Pseudoknotted structures have been predicted to form downstream of putative and established shift sites in

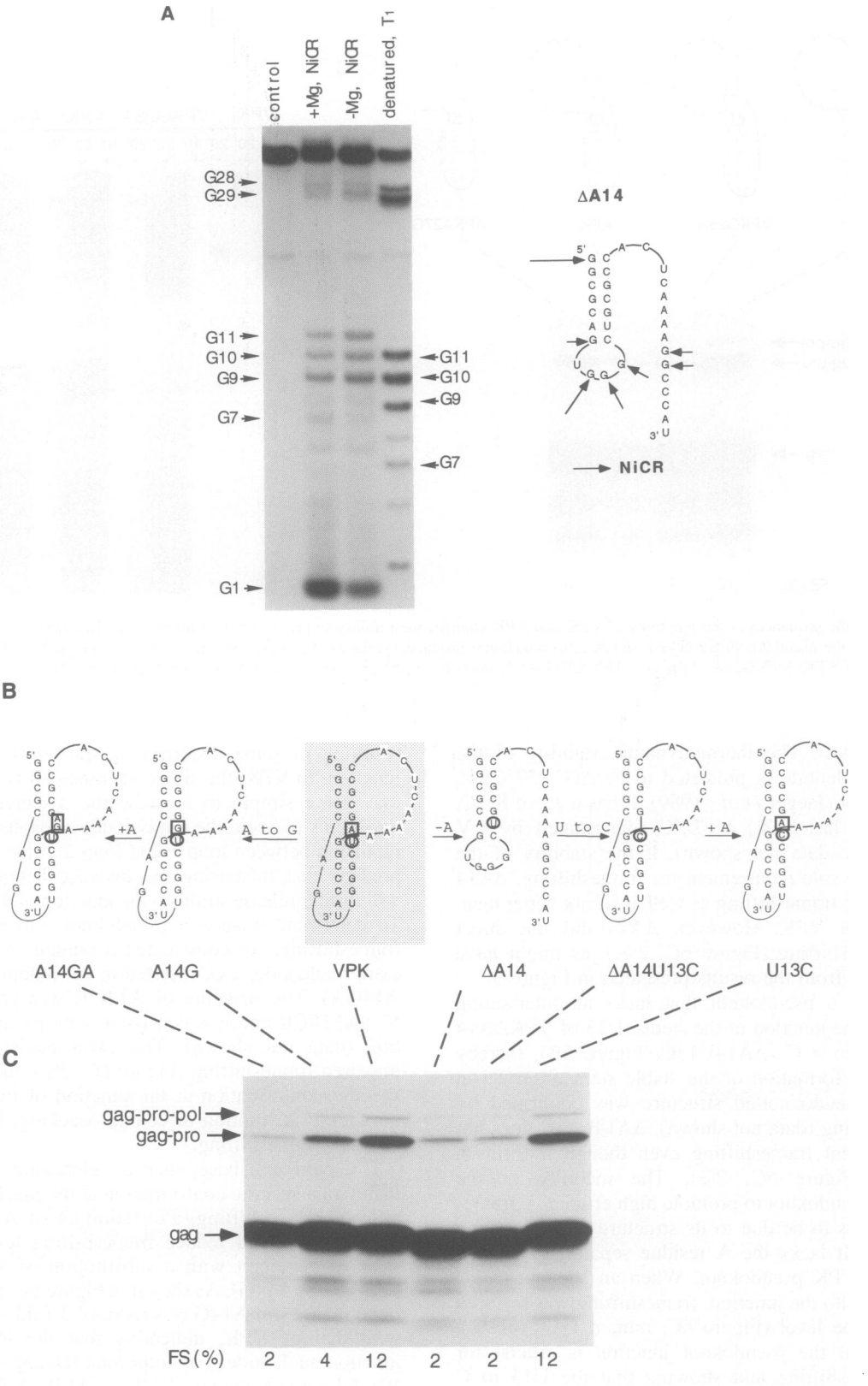

Fig. 6. An intervening A in the junction of VPK is crucial for efficient frameshifting. (**A**) The deletion of A14 in VPK caused a conformational change from a pseudoknot to a 5′ hairpin. Structural mapping of the mutant ΔA14 oligonucleotide with NiCR was carried out as described in Materials and methods. The control lane shows the reaction in the absence of NiCR. (**B**) Point mutations created within the junction region of VPK. The sites of mutations at positions 13 and 14 in VPK are circled (U13) or boxed (A14). (**C**) Frameshifting efficiencies of the mutants of VPK are listed under each lane.

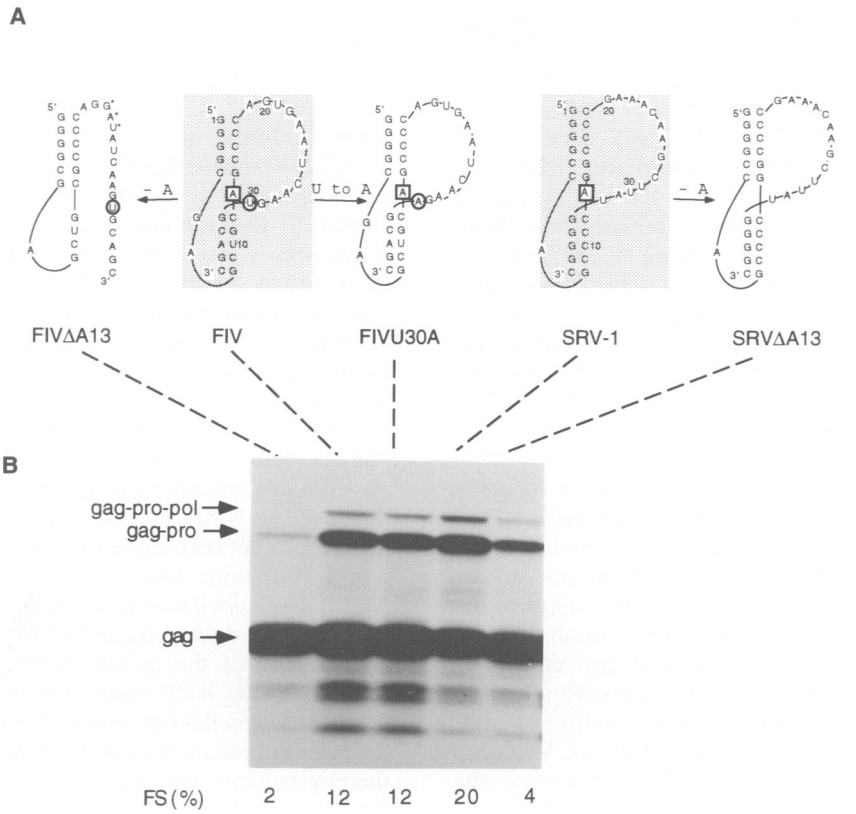

Fig. 7. Other retroviral pseudoknots also cause efficient frameshifting at the MMTV *gag-pro* shift site and appear to have an intervening A at the junction of the stems. (**A**) The proposed secondary structures of pseudoknots derived from FIV and SRV-1 and their mutants. The sites of mutations are circled or boxed as in Figure 6. (**B**) Frameshifting efficiencies of FIV and SRV-1 pseudoknots and their mutants in the context of MMTV *gag-pro* RNA.

various viral RNAs (ten Dam *et al.*, 1990). *In vitro* frameshifting studies have demonstrated that a pseudoknot is required for the −1 frameshifting in the *gag-pol* overlap of the FIV (Morikawa and Bishop, 1992) and in the *gag-pro* overlap of SRV-1 (ten Dam *et al.*, 1994). Although the pseudoknots of FIV and SRV-1 are different from that of MMTV in their primary sequences and in the lengths of stems and loops (Figure 7A), both the FIV and SRV-1 pseudoknots can be folded to display a junction similar to MMTV and the VPK variant, with an intervening A residue interrupting the coaxial stacking of the stems. This junctional conformation requires that the possible base pairing of the intervening A at the junction of the stems with the terminal U in loop 2 does not occur. A G·C pair would then become the first base pair in stem 2. The junctions of the proposed FIV and SRV-1 pseudoknots are exactly the same as the junction of the mutant U13C, which directed frameshifting as efficiently as VPK (Figure 6B and C, 12%). Thus, incorporation of the pseudoknot of SRV-1 and FIV into the MMTV context should promote efficient frameshifting. As predicted, the FIV pseudoknot worked as well as VPK in promoting frameshifting (Figure 7B, 12%) and the SRV-1 pseudoknot actually directed higher frameshifting levels than VPK (Figure 7B, 20%). Furthermore, S_1 and V_1 mapping of the FIV and SRV sequences in the MMTV mRNA context is consistent with pseudoknot formation (data not shown).

If, as we suggest, A13 in the junction region of FIV (Morikawa and Bishop, 1992) or SRV-1 (ten Dam *et al.*, 1990) is not actually base paired with the terminal U in loop 2, mutations predicted to disrupt this base pairing interaction should not impair the function of the pseudoknot in frameshifting. A mutation changing the U30 to an A in FIV (Figure 7A, FIVU30A) did not affect frameshifting (Figure 7B, 12%), indicating that the U30·A13 base pairing is not crucial for the function. Although there is no structural evidence for whether the U30·A13 base pair forms, it is more likely that this relatively weak base pair (compared with a G·C pair) does not form, thus leaving an unpaired A as in VPK. On the other hand, deletion of the A at the junction should impair the function of FIV and SRV-1 pseudoknots, as seen in VPK. Consistent with this prediction, deleting the A in the junction of FIV (Figure 7A, FIVΔA13) and SRV (Figure 7A, SRVΔA13) severely reduced the frameshifting levels to 2 and 4%, respectively (Figure 7B). S_1 and V_1 mapping revealed that in the case of FIV deletion of the intervening A resulted in a conformational change from a pseudoknot to a 5′ hairpin, as described for VPKΔA14; in the case of SRV, however, the pseudoknotted conformation was maintained when A13 was deleted (data not shown).

Discussion

Pseudoknots have been documented to occur in virtually all classes of RNA, where they play important roles

such as interactions with components of the translational apparatus (for recent reviews see Schimmel, 1989; ten Dam *et al.*, 1992). Mutational studies have suggested that pseudoknots form downstream of the −1 frameshift site of the retroviruses (MMTV, FIV and SRV-1), the coronaviruses (IBV and MHV), the torovirus (BEV) and the yeast dsRNA viruses, and that the pseudoknotted structures are required for ribosomal frameshifting. However, there is no direct structural evidence for the formation of pseudoknotted structures in these viral RNAs. The only structural studies of pseudoknots are from direct biochemical probing of the pseudoknot of turnip yellow mosaic virus RNA (Mans *et al.*, 1992), and from biochemical and NMR studies of synthetic RNA oligonucleotides of pseudoknots (Puglisi *et al.*, 1990; Wyatt *et al.*, 1990). Spectroscopic studies by Puglisi *et al.* (1990) revealed the predicted coaxial stacking of the two stems to form a quasi-continuous A-form RNA helix (Pleij and Bosch, 1989). Although the mechanism by which pseudoknots cause frameshifting is unclear, our studies demonstrate that specific tertiary structural features of the pseudoknot are important for ribosomal frameshifting.

We have used site-specific chemical and enzymatic probes to demonstrate that the 34 nucleotide sequence seven nucleotides downstream of the *gag-pro* −1 shift site in MMTV, as well as the variant sequence VPK, are both able to fold into pseudoknotted RNA structures. The nuclease cleavage pattern of the VPK pseudoknot is consistent with a pseudoknotted RNA conformation (Figure 2). The conformation-sensitive chemical probe, NiCR, revealed that the predicted G7·U34 base pair in the VPK pseudoknot did not form (Figure 2), thus allowing two nucleotides to cross the deep major groove of stem 2. This structural feature is also supported by NMR results in which exchangeable imino protons of G7, U8 and U34 were not protected from fast exchange with the solvent (unpublished results). The short loop 1 (two nucleotides) of VPK is in agreement with the predictions based solely on distance between phosphates in an A-form RNA helix (Pleij *et al.*, 1985). According to structural and thermodynamic studies of synthetic RNAs, decreasing loop size favors a hairpin conformation to a pseudoknot (Wyatt *et al.*, 1990). This is supported by our observations with mutant ΔA14: A6 base pairs with U13, shortening loop 1 to one nucleotide and changing the RNA conformation from a pseudoknot to a 5′ hairpin (Figure 6A). Albeit more stable than the corresponding pseudoknot, the hairpin in ΔA14 did not promote efficient frameshifting (Figure 6B and C). This result is consistent with observations reported previously that a stable hairpin is not sufficient to promote efficient frameshifting (Brierley *et al.*, 1991).

APK, a mutated form of VPK with slightly altered base pairing in stem 2, did not direct efficient frameshifting. Structural comparison of VPK and APK revealed major differences in conformation at the junction between stems 1 and 2 (Figure 4). The extensive S_1 cleavage at U13 and A14 in APK indicates that these nucleotides at the junction are ss. Comparison with NMR data on APK and VPK (unpublished results) confirms that the predicted A27·U13 base pair does not form, making the junction more accessible to S_1. Thus, while both VPK and APK fold into pseudoknotted conformations, they have different structural features at the junction. Moreover, VPK promotes −1 frameshifting at 6-fold higher levels than does APK. Finally, the mutations that exchange the primary sequence at the junction regions of VPK and APK (mutants VPKG28A and APKA27G) confer upon each the frameshifting ability of the other. Structural mapping of VPKG28A and APKA27G in the context of the mRNA indicated that both mutants form pseudoknotted structures similar to their parent molecules. The only significant differences were at the junction of the stems where a decreased accessibility to S_1 cleavage correlated with efficient frameshifting. These results suggest that the elements that permit the ribosome to recognize the pseudoknot must be embedded within either the nucleotide sequence at the junction of the pseudoknot or subtle structural variations that exist in the junction region. High-resolution structural studies for VPK and APK are currently underway using multinuclear and multiple-dimensional NMR to determine the detailed structural differences between these two pseudoknots.

It is intriguing that a mutant of VPK lacking A14, ΔA14U13C, albeit having adopted a pseudoknot conformation, did not direct efficient frameshifting. Furthermore, the function of the pseudoknot was rescued by simply reinstalling the intervening nucleotide A in the junction region between the two stems. Deleting the adenine in the junction is predicted to draw stem 1 and stem 2 closer, thereby increase the coaxial stacking interactions of the two stems to form a quasi-continuous helix. Perhaps this kind of close stacking may be detrimental to −1 ribosomal frameshifting. In fact, frameshifting was almost abolished (Figure 3A and B) when the wild-type pseudoknot in MMTV was replaced by the structurally well-characterized pseudoknot PK5 in which the two stems are coaxially stacked (Puglisi *et al.*, 1990). These observations strongly support the hypothesis that a non-coaxially stacked junction of the pseudoknot is crucial for efficient frameshifting. In line with this suggestion, retroviruses that frameshift efficiently, such as FIV and SRV-1, also appear to have pseudoknots with an intervening A nucleotide at the junction between the two stems. The FIV and SRV-1 pseudoknots, when introduced into the analogous position in MMTV mRNA, direct efficient frameshifting (Figure 7). Deletion of the A at the junction of these pseudoknots also diminishes frameshifting, again consistent with a model in which a common structural determinant, the junction region of the pseudoknot, is crucial for pseudoknot-promoted frameshifting.

Two general mechanistic roles can be proposed for the pseudoknot in frameshifting. First, the pseudoknot may present a unique structure that is resistant to the unwinding of a ribosome-associated helicase, thereby causing the ribosome to pause at the shift site. The role of a pseudoknot as a thermodynamically stable 'roadblock' to an approaching ribosome seems too simplistic in the light of our observations and others (Brierley *et al.*, 1991) that stable hairpins, a tRNA with a compact tertiary structure, or a model pseudoknot, PK5, did not direct efficient frameshifting (Figure 3). These results indicate that specific structural features of the pseudoknot determine its function. A second possibility is that the pseudoknot binds to a component of the translational apparatus, causing the ribosome to slip into the −1 reading frame. Our mutational studies of the MMTV pseudoknot uncovered no specific

sequence requirement in the stems and loops of the pseudoknot (Chamorro *et al.*, 1992). However, the fact that a specific type of pseudoknot junction with an intervening nucleotide is required to promote efficient frameshifting suggests that the junction either provides a recognizable binding motif or changes the overall geometry of the pseudoknot to a conformation required for interaction. It has been recognized that bulges and internal loops increase the deformability or bendability of the RNA duplex, and this may present the RNA in a particular conformation required for protein binding at lower free energy (Steitz, 1993). Furthermore, the conformational change modulated by the bulge sequences to disrupt the coaxial stacking of the RNA helix can open up the major groove to interact with proteins (Weeks and Crothers, 1993).

Our results underscore the importance of a particular structure, especially in the junction region between the two helices, in determining the ability of pseudoknots to promote high-level ribosomal frameshifting. It is conceivable that a pseudoknot with this specific conformation may be more resistant to unwinding by ribosome-associated helicases, thereby more effectively stalling the ribosome. On the other hand, the pseudoknot may be recognized by a specific component of the translational apparatus, e.g. the ribosome or an elongation or regulatory factor in the rabbit reticulocyte lysate. This factor would be predicted to interact with the pseudoknot only in the context of the active ribosome, since competition experiments in which increasing amounts (up to 100 μM) of pseudoknot oligonucleotide (VPK) were added to the *in vitro* translation mixture failed to inhibit frameshifting (unpublished results). It has been well documented, especially in prokaryotes, that pseudoknots in several translationally regulated mRNAs bind to ribosomal proteins, such as bacteriophage T4 gene 32 mRNA (Shamoo *et al.*, 1993), *E.coli* S15 mRNA (Philippe *et al.*, 1993) and the α operon of *E.coli* (Tang and Draper, 1989). Further elucidation of the mechanism of pseudoknot-promoted frameshifting in retroviruses would benefit from structural information about the pseudoknot at the atomic level (e.g. from our ongoing studies with NMR spectroscopy) and from attempts to define translational cofactors that might interact with pseudoknots in mRNA (e.g. a genetic screen for modulators of frameshifting efficiency).

Materials and methods

Construction of the mutagenesis cassette

Plasmid pMGPP contains the MMTV *gag*, *pro* and *pol* genes fused to the 5′ portion of RSV *gag* downstream of an SP6 promoter. A unique *Bst*BI site was introduced into the spacer between the shift site and the pseudoknot and a unique *Sna*BI (or *Bsi*WI) site was introduced five nucleotides downstream of the pseudoknot. Subsequent pseudoknot mutants were constructed by subcloning synthetic oligonucleotide fragments into the *Bst*BI and *Sna*BI sites.

−1 frameshifting assay

The mutant MMTV plasmid DNAs were linearized with *Bgl*II and transcribed *in vitro* by SP6 RNA polymerase from the cleaved template (Chamorro *et al.*, 1992). The RNA was translated in rabbit reticulocyte lysates (Promega) and the [^{35}S]methionine-labeled proteins were analyzed by 10% SDS−PAGE. The relative amounts of gag translation products were quantified by a PhosphorImager (Molecular Dynamics) and corrected for differential methionine content of the products.

Structural mapping of pseudoknots in the context of MMTV mRNA

The SP6 transcription mixture containing ~0.5 μg of the 2.6 kb MMTV mRNA was added to S_1 buffer (5 mM Tris−HCl, pH 8.0, 5 mM $MgCl_2$, 60 mM NaCl) or to V_1 buffer (5 mM Tris−HCl, pH 6.3, 5 mM $MgCl_2$, 60 mM NaCl) to a total volume of 150 μl. 50 μl were removed from each mixture and extracted with phenol/chloroform after 20 min at 25°C. To the remaining 100 μl either nuclease S_1 (220 U; Pharmacia) or V_1 (5 U; Pharmacia) was added and incubated at 25°C for either 10 or 20 min, then quenched by phenol-chloroform (50 μl) extraction and the RNA precipitated in 70% ethanol. A 21 oligonucleotide primer 48 nucleotides downstream from the pseudoknot was 5′ end-labeled with [γ-^{32}P]ATP and T4 kinase, then purified by passage through a P10 minicolumn. The S_1- and V_1-digested mRNA was lyophilized and dissolved in 5 μl of annealing buffer (50 mM Tris−HCl, 10 mM DTT) containing ~10 ng (10^6 c.p.m.) of the 5′-labeled primer. The mixture was heated at 82°C for 2 min and incubated at 37°C for 15 min, then chilled on ice. The primer extension was carried out by mixing 3 μl of solution containing AMV RT and dNTPs (3 U, 400 μM each) with 2 μl of annealed mix, incubating at 37°C for 20 min, and quenching with 5 μl of stop buffer (20 mM EDTA, 0.05% bromophenol blue and 0.05% xylene cyanol FF in 95% formamide). The products were then heated at 85°C for 3 min and fractionated on a 6% denaturing polyacrylamide gel.

Synthesis of RNA oligonucleotides

RNA oligonucleotides were synthesized using T7 RNA polymerase and a synthetic ssDNA template with a ds promoter region as described (Puglisi *et al.*, 1990). The full-length transcripts were isolated from a denaturing 20% polyacrylamide gel and electroeluted from the gel. The sequence was confirmed by partial digestion of 5′-^{32}P-labeled transcripts with base-specific RNases.

Enzymatic mapping of RNA oligonucleotides

The structures of 5′-^{32}P-labeled RNA oligonucleotides were probed using nuclease S_1 and ribonuclease V_1 as described (Wyatt *et al.*, 1990). RNase T_1 digestions were carried out for 10 min on ice in 10 μl of 10 mM Tris−HCl, pH 7.0, 100 mM KCl, 10 mM $MgCl_2$ using 0.001 U RNase T_1 (CalBiochem). The reactions were stopped by the addition of 10 μl 9 M urea, 0.05% (w/v) xylene cyanol in 1× TBE (50 mM Tris−HCl, pH 8.1, 50 mM boric acid, 1 mM EDTA) and freezing at −70°C before fractionating on a 20% polyacrylamide gel.

Structural mapping of RNA oligonucleotide with NiCR

5′-^{32}P-labeled RNA in 20 μl of 10 mM potassium phosphate, pH 7.0, 100 mM NaCl, 10 mM $MgCl_2$ and 2 μg unfractionated yeast tRNA were heated at 85°C for 30 s, then slowly cooled to 22°C. NiCR (3 μM) and an oxidant (200 μM), $KHSO_5$, were added to the RNA aliquot and incubated at 22°C for 30 min. The reactions were quenched by adding a solution (180 μl) containing 0.3 M sodium acetate, 10 mM Tris−HCl, pH 7.5, 10 mM EDTA and 3 μg carrier yeast tRNA, extracting with phenol-chloroform (200 ml) and precipitating with ethanol. The precipitated RNA was subsequently redissolved in 1 M aniline acetate (pH 4.5, 20 μl) and incubated at 60°C for 20 min in the dark. The samples were lyophilized, redissolved in water (30 μl) and lyophilized again. The samples were dissolved in 10 μl of gel loading buffer (7 M urea, 0.05% xylene cyanol in 1× TBE) and loaded onto a 20% polyacrylamide gel (7 M urea).

Acknowledgements

We acknowledge David Koh for synthesizing DNA oligonucleotides and Barbara Dengler for general assistance (University of California, Berkeley). We also thank Kevin Luehke, Kung-Yao Chang, Hal Lewis, Marco Molinaro and members of the Varmus Laboratory (especially Michael Chastain, Neil Parkin, Supriya Shivakumar, Hans-Peter Müller and Lucy Godley) for advice and useful discussions. X.C. is supported by a postdoctoral fellowship from the Cancer Research Fund of Damon-Runyon-Walter Winchell Foundation (DRG 1249). S.I.L.is supported by a postdoctoral fellowship from the Jane Coffin Childs Memorial Fund. H.E.V. is an American Cancer Society Research Professor. This research was supported in part by NIH grant GM10840 and DOE grant DE-FG03-86ER60406 (to I.T.) and by NIH grant CA12705 (to H.E.V.).

References

Atkins,J.F., Weiss,R.B. and Gesteland,R.F. (1990) *Cell*, **62**, 413–423.

Bredenbeek,P.J., Pachuk,C.J., Noten,J.H.F., Charite,J., Luytjes,W., Weiss, S.R. and Spaan,W.J.M. (1990) *Nucleic Acids Res.*, **18**, 1825–1832.

Brierley,I., Digard,P. and Inglis,S.C. (1989) *Cell*, **57**, 537–547.

Brierley,I., Rolley,N.J., Jenner,A.J. and Inglis,S.C. (1991) *J. Mol. Biol.*, **229**, 889–902.

Chamorro,M., Parkin,N. and Varmus,H.E. (1992) *Proc. Natl Acad. Sci. USA*, **89**, 713–717.

Chen,X., Burrows,C.J. and Rokita,S.E. (1992) *J. Am. Chem. Soc.*, **114**, 322–325.

Chen,X., Woodson,S.A., Burrows,C.J. and Rokita,S.E. (1993) *Biochemistry*, **32**, 7610–7616.

Clare,J. and Farabaugh,P.J. (1985) *Proc. Natl Acad. Sci. USA*, **82**, 2829–2833.

Craigen,W.J. and Caskey,C.T. (1987) *Cell*, **50**, 1–2.

den Boon,J.A., Snijder,E.J., Chirnside,E.D., de Vries,A.A.F., Horzinek, M.C. and Spaan,W.J.M. (1991) *J. Virol.*, **65**, 2910–2920.

Dinman,J.D., Icho,T. and Wickner,R.B. (1991) *Proc. Natl Acad. Sci. USA*, **88**, 174–178.

Flower,A.M. and McHenry,C.S. (1990) *Proc. Natl Acad. Sci. USA*, **87**, 3713–3717.

Hatfield,D.L., Levin,J.G., Rein,A. and Oroszlon,S. (1992) In Maramorosch,F., Murphy,F. and Shatkin,A. (eds), *Advances in Virus Research*. Academic Press Inc., Orlando, FL, Vol. 4, pp. 193–239.

Herold,J. and Siddell,S.G. (1993) *Nucleic Acids Res.*, **21**, 5838–5842.

Jacks,T. (1990) *Curr. Top. Microbiol. Immunol.*, **157**, 93–124.

Jacks,T., Madhani,H.D., Masiarz,F.R. and Varmus,H.E. (1988) *Cell*, **55**, 447–458.

Jaeger,J.A., Turner,D.H. and Zuker,M. (1989) *Proc. Natl Acad. Sci. USA*, **87**, 7706–7710.

Le,S.-Y., Chen,J.-H. and Maizel,J.V. (1989) *Nucleic Acids Res.*, **15**, 6143–6152.

Mans,R.M.W., Van Steeg,M.H., Verlaan,P.W.G., Pleij,C.W.A. and Bosch,L. (1992) *J. Mol. Biol.*, **223**, 221–232.

Mellor,J., Fulton,S.M., Dobson,M.J., Wilson,W., Kingsman,S.M. and Kingsman,A.J. (1985) *Nature*, **313**, 243–246.

Milligan,J.F., Groebe,D.R., Witherell,G.W. and Uhlenbeck,O.C. (1987) *Nucleic Acids Res.*, **15**, 8783–8798.

Morikawa,S. and Bishop,D.H.L. (1992) *Virology*, **186**, 389–397.

Philippe,C., Eyermann,F., Benard,L., Portier,C., Ehresmann,B. and Ehresmann,C. (1993) *Proc. Natl Acad. Sci. USA*, **90**, 4394–4398.

Pleij,C.W.A. and Bosch,L. (1989) *Methods Enzymol.*, **180a**, 289–303.

Pleij,C.W.A., Rietveld,K. and Bosch,L. (1985) *Nucleic Acids Res.*, **13**, 1717–1731.

Puglisi,J.D., Wyatt,J.R. and Tinoco,I.,Jr (1988) *Nature*, **331**, 283–286.

Puglisi,J.D. and Tinoco,I.,Jr (1989) *Methods Enzymol.*, **180**, 304–325.

Puglisi,J.D., Wyatt,J.R. and Tinoco,I.,Jr (1990) *J. Mol. Biol.*, **214**, 437–453.

Sampson,J.R. and Uhlenbeck,O.C. (1988) *Proc. Natl Acad. Sci. USA*, **85**, 1033–1037.

Schimmel,P. (1989) *Cell*, **58**, 9–12.

Sekine,Y. and Ohtsubo,E. (1989) *Proc. Natl Acad. Sci. USA*, **86**, 4609–4613.

Shamoo,Y., Tam,A. and Konigsberg,W.H. (1993) *J. Mol. Biol.*, **232**, 89–104.

Snijder,E.J., den Boon,J.A., Bredenbeek,P.J., Hirzinek,M.C., Rikinbrand, R. and Spaan,W.J.M. (1990) *Nucleic Acids Res.*, **18**, 4535–4542.

Somogyi,P., Jenner,A.J., Brierley,I. and Inglis,S.C. (1993) *Mol. Cell. Biol.*, **13**, 6931–6940.

Steitz,T.A. (1993) In Gesteland,R.F. and Atkins,J.F. (eds), *The RNA World*. Cold Spring Harbor Laboratory Press, Cold Spring Harbor, NY, pp. 219–237.

Stern,S., Moazed,D. and Noller,H.F. (1988) *Methods Enzymol.*, **164**, 481–489.

Tang,C.K. and Draper,D.E. (1989) *Cell*, **57**, 531–536.

ten Dam,E.B., Pleij,C.W.A. and Bosch,L. (1990) *Virus Genes*, **4**, 121–136.

ten Dam,E., Pleij,K. and Draper,D. (1992) *Biochemistry*, **31**, 11665–11676.

ten Dam,E., Brierley,I., Inglis,S. and Pleij,C. (1994) *Nucleic Acids Res.*, **22**, 2304–2310.

Tsuchihashi,Z. (1991) *Nucleic Acids Res.*, **19**, 2457–2462.

Tsuchihashi,Z. and Kornberg,A. (1990) *Proc. Natl Acad. Sci. USA*, **87**, 2516–2520.

Tu,C., Tzeng,T.-H. and Bruenn,J.A. (1992) *Proc. Natl Acad. Sci. USA*, **89**, 8636–8640.

Tzeng,T.-H., Tu,C. and Bruenn,J.A. (1992) *J. Virol.*, **66**, 999–1006.

van Belkum,A., Verlaann,P., Kun,J.B., Pleij,C.W.A. and Bosch,L. (1988) *Nucleic Acids Res.*, **16**, 1931–1950.

Weeks,K.M. and Crothers,D.M. (1993) *Science*, **261**, 1574–1577.

Wyatt,J.R., Puglisi,J.D. and Tinoco,I.,Jr (1990) *J. Mol. Biol.*, **214**, 455–470.

Wyatt,J.R., Chastain,M. and Puglisi,J.D. (1991) *BioTechniques*, **11**, 764–769.

Received on September 19, 1994; revised on November 18, 1994